Pure & Appl. Chem., Vol. 68, No. 11, pp. 2137–2144, 1996.
Printed in Great Britain.

How do the energetics of the stereoelectronic gauche and anomeric effects modulate the conformation of nucleos(t)ides?

J. Plavec, C. Thibaudeau & J. Chattopadhyaya*

Department of Bioorganic Chemistry, Box 581, Biomedical Centre,
Uppsala University, S-751 23 Uppsala, Sweden

Abstract: The determination of the energetics of the temperature-dependent two-state N ⇄ S pseudorotational equilibrium through $^3J_{HH}$ analysis in 36 nucleos(t)ides and 3 abasic sugars has allowed us for the first time to quantify the strength of various nucleobase-dependent anomeric and gauche effects, and how their interplay finally steers the sugar conformation. The plots of the pD-dependent thermodynamics have given an independent method for the determination of pK_as of all naturally-occurring nucleobases showing that the energetics for the protonation ⇄ deprotonation equilibrium is indeed transmitted through the anomeric effect to drive the two-state N ⇄ S pseudorotational equilibrium (energy pump). This means that any change of the pK_a of a specific nucleobase due to DNA/RNA folding, or H-bonding or any site-specific metal-ion complexation would promote specific local change of DNA/RNA conformation by transmission of the energetics of the altered aromatic character of the heterocyclic agycone to steer the sugar-phosphate backbone conformation through the tuning of the strength of anomeric effect.

The pseudorotation concept was introduced to describe the continuous interconversions of puckered forms of the cyclopentane ring (1). The furanose geometry is described by the phase angle of pseudorotation (P) and the puckering amplitude (Ψ_m) (2). A statistical analysis of X-ray crystal structures of nucleosides and nucleotides has shown that North (N) [0° < P < 36°] and South (S) [144° < P < 190°] conformations are the most dominant forms, which has been the basis of the assumption of the two-state N ⇄ S pseudorotational equilibrium in solution (2,3).

Fig. 1

North (N) sugar (C_3'-*endo*-C_2'-*exo*) South (S) sugar (C_2'-*endo*-C_3'-*exo*)

The conformational behaviour of the pentofuranose moieties in nucleos(t)ides in solution can be understood, quantified and predicted by the relative strengths of gauche and anomeric effects (4). In 2'-deoxyribonucleosides, the 5'-OH and 3'-OH are in energetically preferred gauche orientation with O4', whereas three additional torsion angles Φ[O4'-C1'-C2'-O2'], Φ[O2'-C2'-C3'-O3'] and Φ[O2'-C2'-C1'-N] also prefer gauche conformations in ribonucleosides. The anomeric effect in nucleos(t)ides is the tendency of one of the lone pairs on furanose oxygen to orient antiperiplanar to the glycosidic bond and results in the preference for N-type (pseudoaxial aglycone) over S-type (pseudoequatorial aglycone) conformation (Fig. 1). In crystal structures of natural *N*-nucleosides, the C4'-O4' bond is about 0.03 Å longer than the C1'-O4' bond (3b). The origin of the O-C-N anomeric effect in nucleosides and nucleotides can be described by (i) the higher electrostatic repulsions resulting from unfavourable dipole-dipole interactions which may destabilise the pseudoequatorial orientation (S-type sugar) of the aglycone at C1', or/and (ii) a favourable overlap between a filled n electron pair orbital of the endocyclic O4' and the vacant antibonding σ* orbital of the glycosidic bond which results in the stabilisation of the pseudoaxially oriented nucleobase (N-type sugar) in terms of molecular orbital theory. The latter alternative corresponds to a hyperconjugation of one of the endocyclic oxygen (O4') lone pairs to the glycosidic bond in valence bond theory (double-bond/no-bond resonance form) resulting in the shortening of the endocyclic O4'-C1' bond and the increase of O4'-C1'-N bond angle.

The present report details the summary of our work (4) on the quantitative energetic assessment of various gauche and anomeric effects that determine the N ⇄ S pseudorotational equilibrium. We have used temperature-dependent endocyclic $^3J_{HH}$ coupling constants between 278 K and 358 K to determine the relative population of the N- and S-

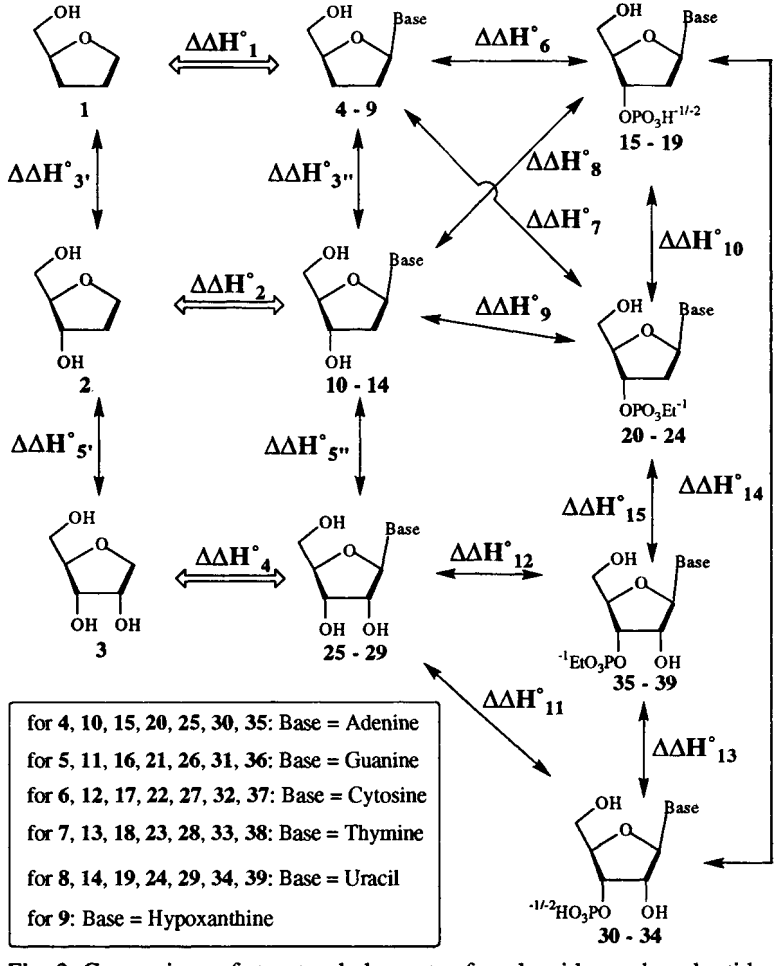

Fig. 2. Comparison of structural elements of nucleosides and nucleotides

TABLE 2. The pairwise correlations of structural features of **1** - **39** with the respective ΔH° values of their N ⇄ S pseudorotational equilibria

Energy	Adenine	Guanine	Cytosine	Thymine	Uracil
$\Delta\Delta H^\circ_1$	4.4	4.4	7.6	5.0	5.3
$\Delta\Delta H^\circ_2$	-0.1	1.6	2.9	2.3	3.5
$\Delta\Delta H^\circ_{3"}$	-9.0	-7.3	-9.2	-7.2	-6.3
$\Delta\Delta H^\circ_4$	-5.0	-3.6	2.1	0.9	1.7
$\Delta\Delta H^\circ_{5"}$	-0.4	-0.7	3.7	3.1	2.7
$\Delta\Delta H^\circ_6$	-10.2	-8.9	-11.2	-8.0	-8.4
$\Delta\Delta H^\circ_7$	-10.3	-9.6	-11.6	-8.4	-8.4
$\Delta\Delta H^\circ_8$	-1.2	-1.6	-2.0	-0.8	-2.1
$\Delta\Delta H^\circ_9$	-1.3	-2.3	-2.4	-1.2	-2.1
$\Delta\Delta H^\circ_{10}$	-0.1	-0.7	-0.4	-0.4	0.0
$\Delta\Delta H^\circ_{11}$	-0.3	-1.3	-1.7	-2.2	-0.9
$\Delta\Delta H^\circ_{12}$	-2.3	-2.6	-4.0	-3.8	-3.7
$\Delta\Delta H^\circ_{13}$	-2.0	-1.3	-2.3	-1.6	-2.8
$\Delta\Delta H^\circ_{14}$	0.5	-0.4	4.0	1.7	3.9
$\Delta\Delta H^\circ_{15}$	-1.4	-1.0	2.1	0.5	1.1

(1) $\Delta\Delta H^\circ_1$ = ΔH° of (**4** - **9**) - ΔH° of **1** signifies the strength of anomeric effect driven two-state N⇄ S equilibrium in ddNs (**4** - **9**). (2) $\Delta\Delta H^\circ_2$ = ΔH° of (**10** - **14**) - ΔH° of **2** signifies the competing anomeric effect and gauche effect of 3'-OH. (3) $\Delta\Delta H^\circ_{3'}$ = ΔH° of **2** - ΔH° of **1** = -4.5 kJ mol^{-1} is the strength of 3'-OH gauche effect. (4) $\Delta\Delta H^\circ_{3"}$ = ΔH° of (**10** - **14**) - ΔH° of (**4** - **8**) signifies the mutual dependence of anomeric effect and gauche effect of 3'-OH on the drive of the two-state N⇄ S equilibrium in dNs (**10** - **14**). (5) $\Delta\Delta H^\circ_4$ = ΔH° of (**25** - **29**) - ΔH° of **3** signifies the dependence of anomeric effect and the effects of 2'- and 3'-OH on the drive of theN⇄ S equilibrium in riboNs (**25** - **29**). (6) $\Delta\Delta H^\circ_{5'}$ = ΔH° of **3** - ΔH° of **2** = 4.5 kJ mol^{-1} signifies the strength of the competing gauche effects of [O4'-C4'-C3'-O3'] and [O4'-C1'-C2'-O2'] fragments. (7) $\Delta\Delta H^\circ_{5"}$ = ΔH° of (**25** - **29**) - ΔH° of (**10** - **14**) signifies the dependence of gauche effects of 2'- and 3'-OH on the drive of the two-state N⇄ S equilibrium in riboNs (**25** - **29**). (8) $\Delta\Delta H^\circ_6$ = ΔH° of (**15** - **19**) - ΔH° of (**4** - **8**) signifies the strength of the nucleobase-dependent gauche effects of [O4'-C4'-C3'-3'-monophosphate] fragment on the drive of the two-state N⇄ S equilibrium in dNMPs (**15** - **19**). (9) $\Delta\Delta H^\circ_7$ = ΔH° of (**20** - **24**) - ΔH° of (**4** - **8**) signifies the strength of the nucleobase-dependent gauche effects of [O4'-C4'-C3'-3'-ethylphosphate] fragment. (10) $\Delta\Delta H^\circ_8$ = ΔH° of (**15** - **19**) - ΔH° of (**10** - **14**) signifies the additional stabilization of S-type conformers by 3'-monophosphate compared to 3'-OH in the parent 2'-dNs. (11) $\Delta\Delta H^\circ_9$ = ΔH° of (**20** - **24**) - ΔH° of (**10** - **14**) signifies the additional stabilization of S-type conformers by 3'-ethylphosphate compared to 3'-OH in the parent dNs. (12) $\Delta\Delta H^\circ_{10}$ = ΔH° of (**20** - **24**) - ΔH° of (**15** - **19**) signifies the additional stabilization of S-type conformers by 3'-ethylphosphate compared to 3'-monophosphates. (13) $\Delta\Delta H^\circ_{11}$ = ΔH° of (**30** - **34**) - ΔH° of (**25** - **29**) signifies the additional stabilization of S-type conformers by 3'-monophosphate compared to 3'-OH in parent rNs. (14) $\Delta\Delta H^\circ_{12}$ = ΔH° of (**35** - **39**) - ΔH° of (**25** - **29**) signifies the additional stabilization of S-type conformers by 3'-ethylphosphate compared to 3'-OH in parent rNs. (15) $\Delta\Delta H^\circ_{13}$ = ΔH° of (**35** - **39**) - ΔH° of (**30** - **34**) signifies the additional stabilization of S-type conformers by 3'-ethylphosphate compared to 3'-monophosphate in rNMPs. (16) $\Delta\Delta H^\circ_{14}$ = ΔH° of (**30** - **34**) - ΔH° of (**15** - **19**) signifies the effect of 2'-OH on the drive of the two-state N ⇄ S equilibrium in rNMPs **30** - **34**. (17) $\Delta\Delta H^\circ_{15}$ = ΔH° of (**35** - **39**) - ΔH° of (**20** - **24**) signifies the strength of the effect of 2'-OH···O3'-PO$_3$Et$^-$ H-bonding interactions on the drive of the two-state equilibrium in rNpEts **35** - **39**.

type conformers [(P_N, Ψ_m^N) ⇄ (P_S, Ψ_m^S)] for the van't Hoff plots because of the fact that as the relative populations of N- and S-type pseudorotamers change, their geometries remain unchanged (4). Further evidence for a two-state equilibrium in the van't Hoff plots are the NMR studies which have clearly shown the presence of two distinctly identifiable (by their different chemical shifts and $^3J_{1'2'}$) dynamically interconverting N and S conformations of some sugar moieties owing to their different stereochemical environments in B ⇄ Z DNA (5a) or A ⇄ Z RNA (5a) or A-form ⇄ B-form lariat RNA (5a) transformations as a result of change of the salt or alcohol concentration in the buffer or as a result of change of temperature. Recent work by Raman spectroscopy has also identified a similar two-state equilibrium in A and T-containing DNAs (5b).

Table 1 presents experimental ΔH° and ΔS° values for N⇄ S equilibrium of furanose moieties in **1** - **39**. Our approach consists of pairwise comparisons of structural features of abasic sugars **1** - **3** and 2',3'-dideoxy- (ddNs, **4** - **9**), 2'-deoxy- (dNs, **10** - **14**) and ribonucleosides (riboNs, **25** - **29**) as well as nucleotides **15** - **24** and **30** - **39** shown in Fig. 2. The subtractions of the respective thermodynamic data derived from two sets of compounds (shown by double-headed arrows in Fig. 2) resulting from the temperature-dependent N ⇄ S pseudorotational equilibria enabled us for the first time to determine the strengths of the anomeric and gauche effects (Fig. 2 & Table 2) in a quantitative manner. The accuracy of our procedure and of the resulting thermodynamic data is self-evident from the fact that this protocol enables the determination of pK_as of the heterocyclic aglycones of the nucleosides (see below) within ±0.1 of literature pK_a (6). The summary of our observations (Fig. 3) are as follows:

(A) Energetics of the anomeric effects are dictated by unique aromatic character of the aglycone

(i) The preference of 5'-CH_2OH group to occupy the pseudoequatorial orientation is manifested in the positive ΔH° value for the pseudorotational equilibrium of **1** (Table 1). Subtraction of ΔH° for **1** from those of ddNs **4** - **9** (Table 1) gives $\Delta\Delta H^\circ_1$ (Table 2 & Fig. 2). These show that the combined stereoelectronic and steric contributions in the anomeric effect of the nucleobases increases in the following order: adenine ≈ guanine < thymine < uracil < cytosine. One reason for the stronger anomeric effect in pyrimidine ddNs **6** - **8** than in purine counterparts is that the n(O4')→ $\sigma^*_{C1'\text{-}N}$ delocalization is more effective in the π-deficient pyrimidine moiety compared to relatively more electron-rich purine in ddNs **4**, **5** and **9**. It is however difficult to rule out any potential contribution of dipole-dipole repulsion as the origin of the anomeric effect in the neutral state [see section (x)].

(ii) The ΔH° of N ⇄ S equilibrium of both abasic sugar **2** and dNs **10** - **14** consists of the substituent effect of 5'-CH_2OH and the gauche effect of [O4'-C4'-C3'-O3'] fragment, hence estimation of $\Delta\Delta H^\circ_2$ (Table 2), allows us to show that the anomeric effect in dNs increases in the following order: adenine < guanine < thymine < cytosine < uracil. This is in accordance with the conclusion made on the basis of the comparison of $\Delta\Delta H^\circ_1$ values that pyrimidine nucleosides exhibit stronger anomeric effect than purines. However, the estimates of the strengths of the anomeric effect of individual nucleobases vary considerably between ddNs **4** - **8** and dNs **10** - **14**. The weakening of the anomeric effect in dNs compared to ddNs is due to the change in the electrostatic potential around O4' as it experiences the electron-withdrawing effect of the 3'-OH group. The enhancement of the strength of [O4'-C4'-C3'-O3'] gauche effect in dNs compared to **2**, on the other hand, is due to more effective overlap of σ orbital of C3'-H bond to the σ* of C4'-O4' bond as the O4' electron-density is more reduced with the strengthening of the anomeric effect. It should be noted that the gauche effect of the [O4'-C4'-C3'-O3'] fragment is much stronger than anomeric effect and is responsible for the preference for S-type conformers in dNs **10** - **14** (Table 1).

(iii) The correlation of the thermodynamic data of N ⇄ S equilibrium in riboNs with their constituent structural elements becomes very complex. As [O4'-C4'-C3'-O3'] and [O4'-C1'-C2'-O2'] gauche effects in **3** and riboNs **25** - **29** cancel each other, the subtraction of ΔH° values for abasic sugar **3** from riboNs **25** - **29** gives an estimate for the combined anomeric effect of the nucleobase and the gauche effect of the [N-C1'-C2'-O2'] fragment ($\Delta\Delta H^\circ_4$). The subtraction of the values for the gauche effect of [N-C1'-C2'-O2'] fragment [see section (v)] gives an estimate for the anomeric effect of adenine (+4.4 kJ mol^{-1}), guanine (+4.4 kJ mol^{-1}), cytosine (+7.6 kJ mol^{-1}), thymine (+5.0 kJ mol^{-1}) and uracil (+5.3 kJ mol^{-1}) base in riboNs **25** - **29**. Note, that the strengths of the individual anomeric effects are comparable in ddNs **4** - **8** and riboNs **25** - **29** while they are smaller in dNs **10** - **14** because the anomeric effects in dNs are weakened by 3'-OH, whereas the electron-withdrawing effects of the vicinal 2'-OH and 3'-OH groups on O4' are mutually canceled in riboNs because of inductive effect, σ→ σ* interaction (gauche effect) or H-bonding.

(B) Energetics of the nucleobase-dependent gauche effects drive N ⇄ S equilibrium in pentofuranose moiety

(iv) The comparison of ΔH° values in **1** and **2** suggests that the strength of the gauche effect of [O4'-C4'-C3'-O3'] fragment in the absence of the nucleobase (*i.e.* $\Delta\Delta H^\circ_{3'}$) is -4.5 kJ mol^{-1}. The estimates of the strength of [O4'-C4'-C3'-O3'] gauche effect in dNs **10** - **14** are much higher (*i.e.* $\Delta\Delta H^\circ_{3''}$ values, Table 2), suggesting that the anomeric effect and the gauche effect of 3'-OH with O4' are strongly interrelated.

(v) The comparison of ΔH° values in **2** and **3** suggests that the strength of the gauche effect of [O4'-C1'-C2'-O2'] fragment (*i.e.* $\Delta\Delta H^\circ_{5'}$) is +4.5 kJ mol^{-1}. The ΔH° values are comparable in **1** and **3** (Table 1) which proves that in **3** the gauche effects of [O4'-C1'-C2'-O2'] and [O4'-C4'-C3'-O3'] fragments effectively cancel each other. The

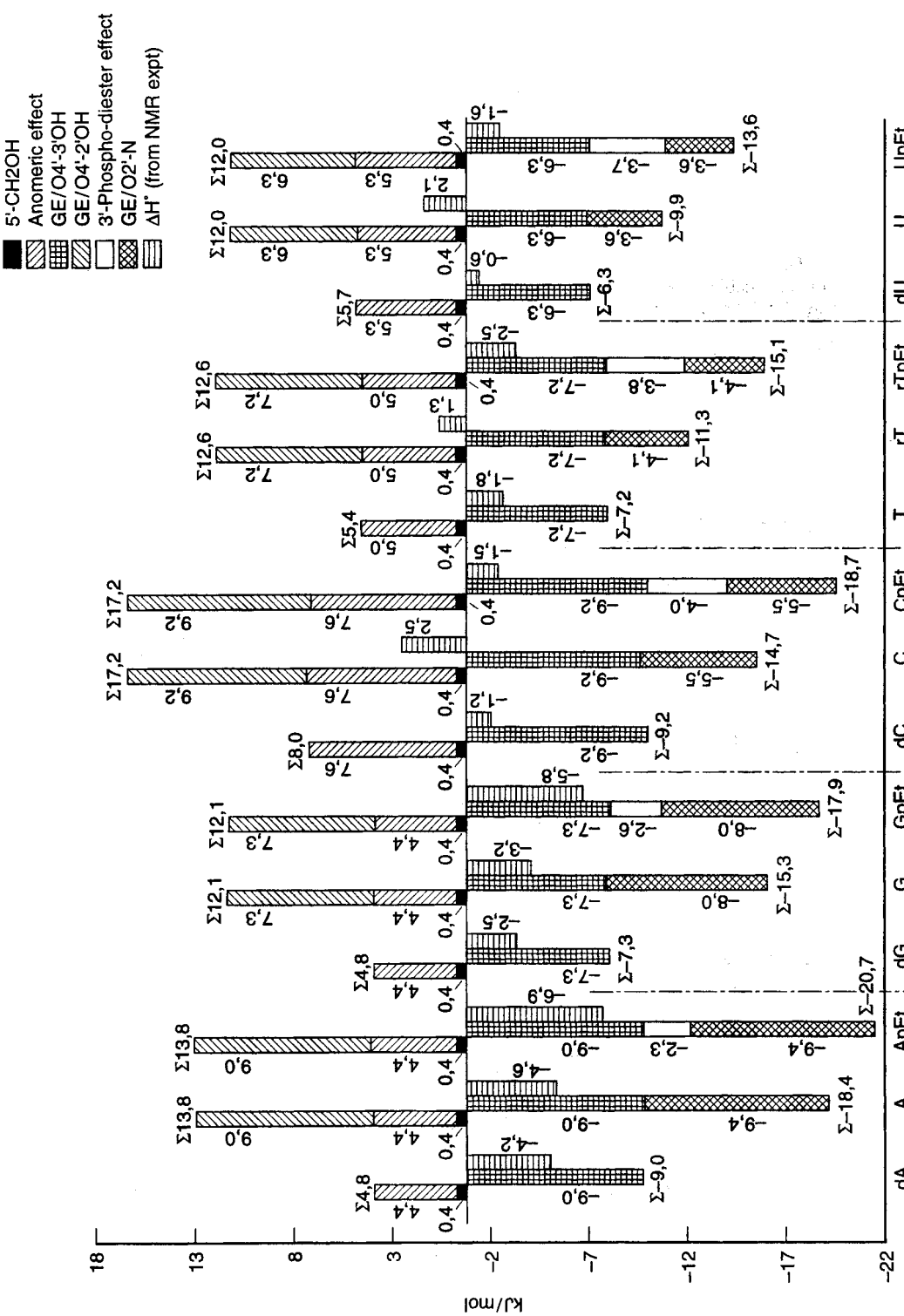

Fig. 3. Dissection of the competing energetics of anomeric and gauche effects in nucleosides and nucleotides (see Fig.2 and Table 2 for pairwise dissection of experimental ΔH° to give nucleobase-specific anomeric and gauche effects)

subtraction of ΔH° in riboNs **25** - **29** from those in dNs **10** - **14** gives $\Delta\Delta H^\circ_{5'}$ values, showing the combined effect of the 2'-OH group and the gauche effects of [O4'-C1'-C2'-O2'] and [N-C1'-C2'-O2'] fragments (Table 2). Subtraction of the gauche effect of [O4'-C1'-C2'-O2'] fragment (since it has been shown that they are of equal strength as the nucleobase-dependent gauche effect of [O4'-C4'-C3'-O3'] fragment, *i.e.* $\Delta\Delta H^\circ_{3'}$) yields the estimate for the [N-C1'-C2'-O2'] gauche effect in riboNs **25** - **29**: -9.4 kJ mol^{-1} in case of adenine as a base, -8.0 kJ mol^{-1} with guanine, -5.5 kJ mol^{-1} with cytosine, -4.1 kJ mol^{-1} with thymine and -3.6 kJ mol^{-1} with uracil (see Fig. 3 for relative contribution of various stereoelectronic effects in nucleos(t)ides).

(vi) The gauche effect of 3'-$OPO_3H^{-1/-2}$ fragment in **15** - **19** ($\Delta\Delta H^\circ_6$) and the gauche effect of 3'-OPO_3Et^- fragment in **20** - **24** ($\Delta\Delta H^\circ_7$) drive the sugar conformation towards S-type by 0.8 to 2.4 kJ mol^{-1} ($\Delta\Delta H^\circ_8$ and $\Delta\Delta H^\circ_9$, Table 2) stronger than 3'-OH in dNs **10** - **14**.

TABLE 1. Thermodynamic data of the N ⇄ S pseudorotational equilibria in **1** - **39**

Compound	ΔH° [a,c]	ΔS° [a,c]	$-T\Delta S^\circ$ [a,c]	ΔG^{298} [a,c]	%S [b] (278 K)	%S [b] (358 K)	Δ%S (358K-278K)
1	0.4 (0.3)	1.1 (1.0)	-0.3	0.1	49	50	1
2	-4.1 (0.3)	-5.0 (0.9)	1.5	-2.6	76	68	-8
3	0.4 (0.1)	-5.1 (3.5)	1.5	1.9	31	32	1
ddA (**4**)	4.8 (0.2)	7.4 (2.1)	-2.2	2.6	23	33	10
ddG (**5**)	4.8 (0.2)	7.2 (0.3)	-2.1	2.7	23	32	9
ddC (**6**)	8.0 (0.4)	15.9 (1.4)	-4.7	3.3	18	32	14
ddT (**7**)	5.4 (0.2)	6.0 (0.8)	-1.8	3.6	17	25	8
ddU (**8**)	5.7 (0.3)	7.0 (1.2)	-2.1	3.6	16	25	9
ddI (**9**)	6.2 (0.2)	9.6 (1.1)	-2.9	3.3	18	28	10
dA (**10**)	-4.2 (0.1)	-6.9 (0.7)	2.1	-2.1	73	64	-9
dG (**11**)	-2.5 (0.1)	-2.6 (0.9)	0.8	-1.7	68	63	-5
dC (**12**)	-1.2 (0.1)	0.1 (1.0)	0.0	-1.2	63	60	-3
T (**13**)	-1.8 (0.3)	-0.9 (0.5)	0.3	-1.5	66	62	-4
dU (**14**)	-0.6 (0.1)	1.5 (0.2)	-0.4	-1.0	61	59	-2
dAMP (**15**)	-5.4 (0.3)	-9.9 (0.7)	3.0	-2.4	76	65	-11
dGMP (**16**)	-4.1 (0.2)	-6.5 (0.7)	1.9	-2.2	73	64	-9
dCMP (**17**)	-3.2 (0.1)	-6.8 (0.5)	2.0	-1.2	64	56	-8
TMP (**18**)	-2.6 (0.1)	-4.3 (0.4)	1.3	-1.3	65	59	-6
dUMP (**19**)	-2.7 (0.1)	-3.8 (0.8)	1.1	-1.6	67	61	-6
dApEt (**20**)	-5.5 (0.2)	-7.9 (0.7)	2.4	-3.1	81	71	-10
dGpEt (**21**)	-4.8 (0.2)	-7.0 (0.7)	2.1	-2.7	77	68	-9
dCpEt (**22**)	-3.6 (0.2)	-5.3 (0.9)	1.6	-2.0	72	64	-8
TpEt (**23**)	-3.0 (0.1)	-3.2 (1.1)	1.0	-2.0	71	65	-6
dUpEt (**24**)	-2.7 (0.2)	-2.3 (0.6)	0.7	-2.0	71	65	-6
A (**25**)	-4.6 (0.4)	-9.5 (0.6)	2.8	-1.8	70	60	-10
G (**26**)	-3.2 (0.2)	-5.5 (0.7)	1.6	-1.6	67	60	-7
C (**27**)	2.5 (0.2)	3.9 (0.9)	-1.2	1.3	35	41	6
rT (**28**)	1.3 (0.1)	4.4 (0.7)	-1.3	0.0	49	52	3
U (**29**)	2.1 (0.2)	6.2 (2.7)	-1.8	0.3	46	51	5
AMP (**30**)	-4.9 (0.4)	-9.1 (0.7)	2.7	-2.2	74	63	-11
GMP (**31**)	-4.5 (0.2)	-10.8 (1.6)	3.2	-1.3	66	55	-11
CMP (**32**)	0.8 (0.2)	-0.6 (1.8)	0.2	1.0	40	42	2
rTMP (**33**)	-0.9 (0.2)	-1.6 (0.9)	0.5	-0.4	55	53	-2
UMP (**34**)	1.2 (0.2)	2.1 (1.2)	-0.6	0.6	43	46	3
ApEt (**35**)	-6.9 (0.8)	-13.6 (1.1)	4.1	-2.8	79	66	-13
GpEt (**36**)	-5.8 (0.4)	-12.3 (1.1)	3.7	-2.1	74	62	-12
CpEt (**37**)	-1.5 (0.2)	-5.3 (1.0)	1.6	0.1	50	47	-3
rTpEt (**38**)	-2.5 (0.3)	-5.3 (1.2)	1.6	-0.9	61	55	-6
UpEt (**39**)	-1.6 (0.1)	-3.1 (0.6)	0.9	-0.7	58	54	-4

[a] ΔH°, $-T\Delta S^\circ$ and ΔG° at 298 K are in kJ mol^{-1} and ΔS° (J K^{-1} mol^{-1}) are the average values (standard deviations are in parentheses, see ref. 4 for the actual protocol). [b] The % S conformer was calculated by %S (T) = 100 * [exp ($-\Delta G^T$/ RT)] / [exp ($-\Delta G^T$/ RT) +1]. [c] The negative or positive values denote the drive to the S- or N-type conformer, respectively.

(vii) The pairwise subtraction of ΔH° values in riboNs **25** - **29** from their corresponding 3'-monophosphates **30** - **34**, respectively, has shown that the S-type pseudorotamers are uniformly stabilized in the latter by -0.3 to -2.2 kJ mol^{-1} ($\Delta\Delta H^\circ_{11}$, Table 2) which is attributed to the stronger gauche effect of [C4'-C3'-O3'-$OPO_3H^{-1/-2}$] fragment compared to that of [C4'-C3'-O3'-OH]. The subtraction of ΔH° for riboNs **25** - **29** from the 3'-ethylphosphate derivatives **35** - **39**, respectively, has shown that the gauche effect of [O4'-C4'-C3'-3'OPO_3Et^-] fragment is stronger

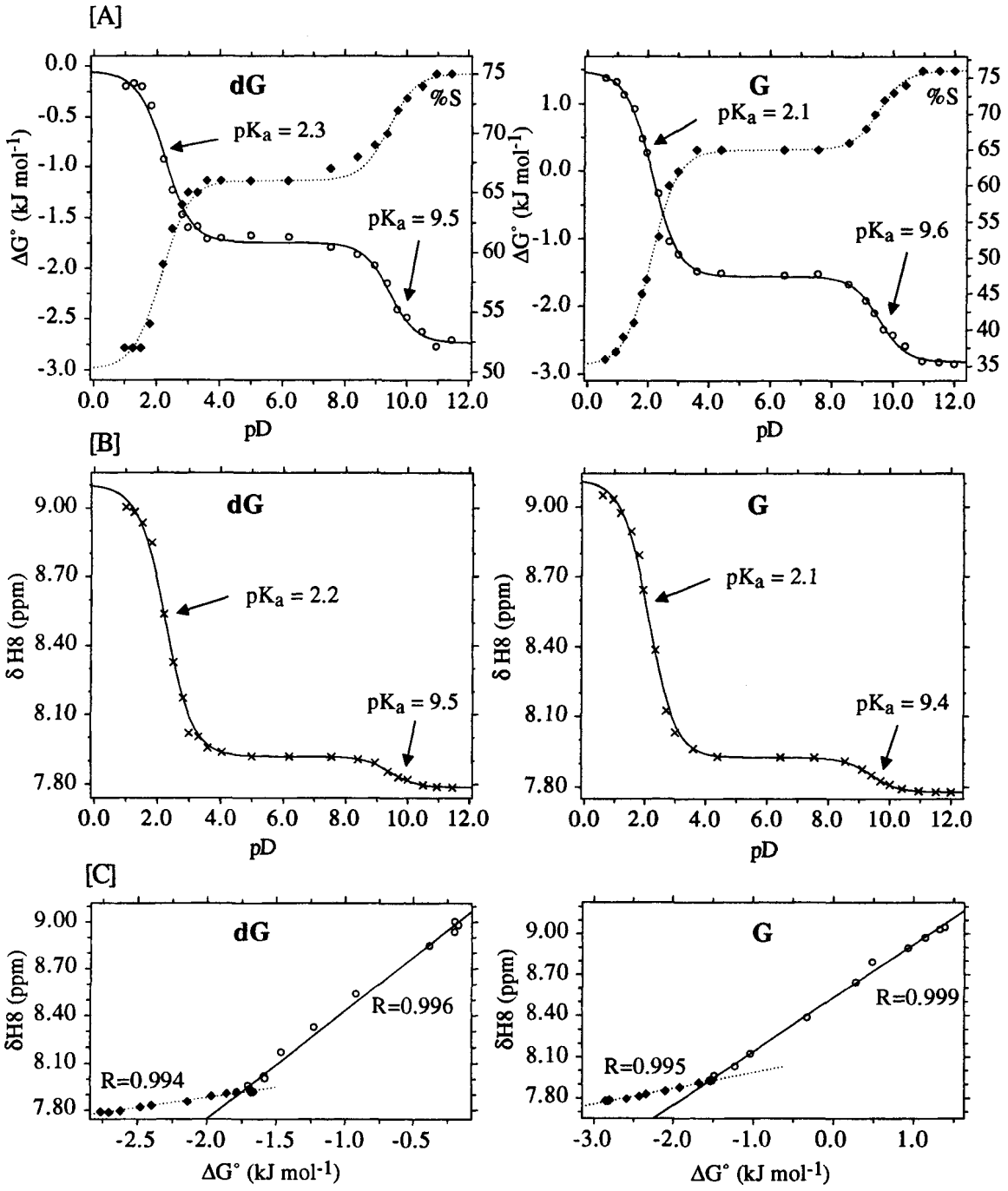

Fig. 4. The estimation of pD-dependent thermodynamics of N⇄ S equilibrium gives a direct measurement of the pK_a of the aglycone and the pD-tunable anomeric effect exemplified (see ref. 4j for details) by dG (**11**) and G (**26**). [A] ΔG° (left ordinate) and %S (right ordinate) at 298 K as a function of pD giving the pK_a of the nucleobase at the inflection point. [B] ^{1}H-NMR chemical shift of δH8 as a function of pD giving the pK_a of the nucleobase at the inflection point. Note the similarity of these titration curves with the ones obtained by pD-dependent ΔG° of N ⇄ S equilibrium shown in panel A. [C] The plot of δH8 *vs.* ΔG° gives a straight line with the Pearson correlation coefficient above 0.99 showing that N ⇄ S equilibrium and the protonation ⇄ deprotonation equilibrium are indeed a correlated event due to transmission of the energetics through the anomeric effect (energy pump).

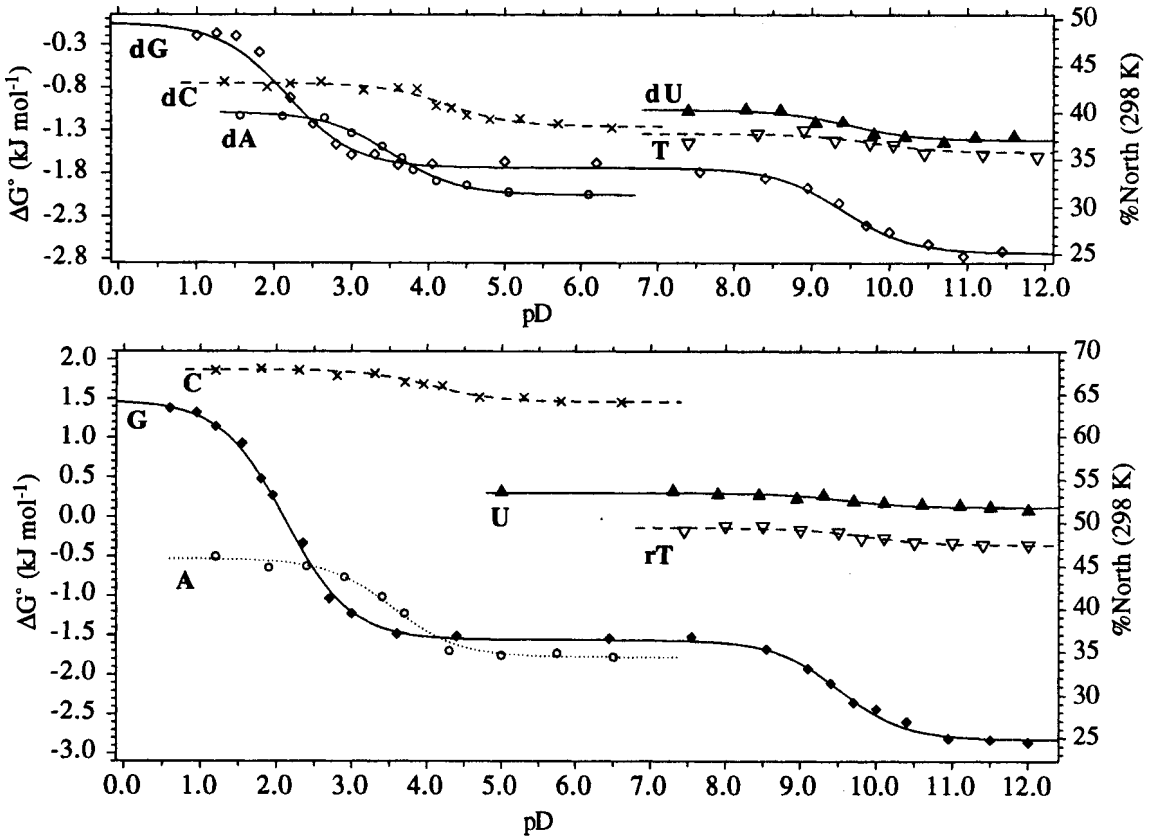

Fig. 5. The experimental ΔG° values at 298 K for the N ⇄ S pseudorotational equilibrium of dNs **10** - **14** and riboNs **25** - **25** as a function of pD. The sigmoidal curves are the best iterative least square fit of the pD-dependent experimental ΔG° values giving the following pK_a (error ±0.1, except for rT and U (±0.2)) of the nucleobase at the inflection point(s): dA (3.5), dG (2.3, 9.5), dC (4.2), T (9.7), dU (9.5), A (3.5), G (2.1, 9.6), C (4.0), rT (9.9) and U (9.6). Note the present pK_as determined using ΔG° values are comparable to the literature pK_as determined potentiometrically or photometrically (6).

TABLE 3. Thermodynamic data of the N ⇄ S equilibrium of **10** - **14** and **25** - **29** with fully protonated, neutral and fully deprotonated nucleobases[a]

Compd	Fully protonated nucleobase			Neutral nucleobase			Fully deprotonated nucleobase			**pD-tunability** of anomeric effect	
	ΔH°_P	$-T\Delta S^\circ_P$	ΔG°_P	ΔH°_N	$-T\Delta S^\circ_N$	ΔG°_N	ΔH°_D	$-T\Delta S^\circ_D$	ΔG°_D	$\Delta\Delta G^\circ_{P\text{-}N}$	$\Delta\Delta G^\circ_{N\text{-}D}$
dA (**10**)	-0.7	-0.4	-1.1	-3.9	1.8	-2.1	-	-	-	1.0	-
dG (**11**)	2.1	-2.2	-0.1	-2.8	1.1	-1.7	-4.9	2.2	-2.7	1.6	2.0
dC (**12**)	0.0	-0.8	-0.8	-0.7	-0.5	-1.3	-	-	-	0.5	-
T (**13**)	-	-	-	-1.4	0.1	-1.3	-1.9	0.3	-1.6	-	0.3
dU (**14**)	-	-	-	-0.6	-0.4	-1.1	-1.3	-0.1	-1.4	-	0.3
A (**25**)	-0.2	-0.4	-0.5	-4.4	2.6	-1.8	-	-	-	1.3	-
G (**26**)	5.4	-4.2	1.5	-3.3	1.8	-1.5	-7.6	4.8	-2.8	3.0	1.3
C (**27**)	5.2	-3.3	1.9	2.3	-0.8	1.5	-	-	-	0.4	-
rT (**28**)	-	-	-	1.3	-1.4	-0.1	-0.2	-0.2	-0.4	-	0.3
U (**29**)	-	-	-	2.0	-1.7	0.3	0.3	-0.2	0.1	-	0.2

[a] The values of ΔH°, -TΔS° (at 298 K) and ΔG° values are given in kJ mol^{-1}. The subscript 'N' denotes the neutral state, subscript 'P' denotes the protonated state and subscript 'D' denotes the deprotonated state. The plateaus found in Fig. 5 in the acidic, neutral and alkaline ranges for ΔH°, ΔS° and ΔG° values were obtained by the iterative nonlinear least-square fitting procedure of the experimental ΔH°, ΔS° and ΔG° values at several individual pDs.

than that of [O4'-C4'-C3'-3'OH] fragment by -2.3 to -4.0 kJ mol^{-1} ($\Delta\Delta H^{\circ}_{12}$, Table 2). It is noteworthy that the relative strengths of the gauche effects of [O4'-C4'-C3'-3'OPO_3Et^-] compared to [O4'-C4'-C3'-3'$OPO_3H^{-1/-2}$] are stronger in the ribo series than in 2'-deoxy counterparts ($\Delta\Delta H^{\circ}_{13} > -1.3$ kJ mol^{-1}, Table 2).

(viii) The overall effect of 2'-OH group on the drive of N ⇄ S pseudorotational equilibrium depends on the nature of vicinal 3'-substituent ($\Delta\Delta H^{\circ}_{14}$ for phosphomonoester and $\Delta\Delta H^{\circ}_{15}$ for phosphodiester function) and varies with the strength of their intramolecular interaction. The reason that 3'-OPO_3Et^- group additionally stabilizes the S-type pseudorotamers compared to 3'-$OPO_3H^{-1/-2}$ counterparts is that the former undergoes specific H-bonding interaction involving 2'-OH···O3'-PO_3Et^- in **35** -**39**.

(C) The energy of the protonation⇄ deprotonation equilibrium of the heterocyclic aglycone is transmitted through the anomeric effect to drive the N ⇄ S pseudorotational equilibrium (Energy pump)

(ix) ΔG° values of the N⇄ S equilibrium of dNs and riboNs show a sigmoidal dependence on the pD (Figs. 4 & 5), characteristic for a typical titration curve with the inflection point corresponding to the pK_a of the heterocyclic base (6), which is identical to the titration curves obtained by pD-dependent aromatic and anomeric chemical shift measurements (Fig. 4B) (4j). The plots of $\delta(^1H)$ *vs.* ΔG° of N ⇄ S equilibrium show straight lines with the Pearson correlation coefficient higher than 0.97 [exemplified in Fig. 4C with the plots for dG (**11**) and G (**26**)]. This means that the thermodynamics of the pD-dependent change of the protonation ⇄ deprotonation equilibrium also drives the N ⇄ S pseudorotational equilibrium (energy pump) by beeing transmitted through the pD-tunable anomeric effect (see Table 3). The reproduction of the known pK_as through ΔG° measurements of the N⇄ S equilibrium also proves the accuracy of the observed thermodynamics shown in Tables 1-3 as well as unambiguously validates the two-state N ⇄ S equilibrium in aqueous solution.

(x) If dipole-dipole repulsion were the main origin of the anomeric effect in nucleosides, then we would have found the weaker anomeric effect in the protonated form and stronger anomeric effect in the anionic form compared to the neutral state. Our experimental result in Fig. 5 actually shows the opposite: the strength of the anomeric effect was enhanced upon protonation (evident by the increase of N-type sugar population) and it was found to be weakened upon deprotonation (evident by the decrease of N-type sugar population) relative to the neutral state. Our results are consistent with the favorable $n(O4')\rightarrow\sigma^*_{C1'\text{-}N}$ delocalization in the electron-deficient protonated-aglycone at the acidic pH, and unfavorable $n(O4')\rightarrow\sigma^*_{C1'\text{-}N}$ delocalization in the electron-rich anionic-aglycone at the basic pH, compared to the neutral state, as the origin of anomeric effect.

(xi) These results suggest that any local change of hydrophobic properties changing the pK_a of a specific nucleobase or H-bonding or any site-specific metal-ion complexation to any nucleobase would promote specific local change of DNA/RNA conformation by transmission of the energetics of the altered aromatic character of the heterocyclic aglycone to steer the sugar-phosphate backbone conformation through the tuning of the strength of anomeric effect. Thus the nucleobase acts as an electronic sensor (beside its H-bonding and stacking ability) of the environmental condition around DNA/RNA to specifically alter a conformation in a certain microsphere, which in turn, can serve as the recognition point for a specific ligand complexation or as a signal for a highly-specific biological function.

Acknowledgments. We thank Swedish Board for Technical Development (NUTEK), Swedish Natural Science Research Council (NFR) for generous financial supports, Wallenbergsstiftelsen and Uppsala University for funds for the purchase of a 500 MHz Bruker AMX NMR spectrometer.

References

1. J.E. Kilpatrick; K.S. Pitzer and R. Spitzer *J. Am. Chem. Soc.* **1947**, *69*, 2483.
2. C. Altona and M. Sundaralingam *J. Am. Chem. Soc.* **1972**, *94*, 8205; **1973**, *95*, 2333.
3. (a) C. Altona; R. Francke; R. de Haan; J.H. Ippel; G.J. Daalmans; A.J.A. Westra Hoekzema and J. van Wijk *Magn. Reson. Chem.* **1994**, *32*, 4123. (b) W. Saenger *Principles of Nucleic Acid Structure* ; Springer Verlag: New York, 1984.
4. (a) J. Plavec; W. Tong and J. Chattopadhyaya *J. Am. Chem. Soc.* **1993**, *115*, 9734. (b) J. Plavec; N. Garg and J. Chattopadhyaya *J. Chem.Soc., Chem. Commun.* **1993**, 1011. (c) J. Plavec; L.H. Koole and J. Chattopadhyaya *J. Biochem. Biophys. Meth.* **1992**, *25*, 253. (d) J. Plavec; C. Thibaudeau; G. Viswanadham; C. Sund and J. Chattopadhyaya *J. Chem. Soc., Chem. Comm.* **1994**, 781. (e) C. Thibaudeau; J. Plavec; K.A. Watanabe and J. Chattopadhyaya *J. Chem. Soc., Chem. Comm.* **1994**, 537. (f) C. Thibaudeau; J. Plavec; N. Garg; A. Papchikhin and J. Chattopadhyaya *J. Am. Chem. Soc.* **1994**, *116*, 4038. (g) J. Plavec; C. Thibaudeau and J. Chattopadhyaya *J. Am. Chem. Soc.* **1994**, *116*, 6558. (h) C. Thibaudeau; J. Plavec and J. Chattopadhyaya *J. Am. Chem. Soc.* **1994**, *116*, 8033. (i) J. Plavec Ph.D. Thesis, Department of Bioorganic Chemistry, Uppsala University, Sweden, **1995**. (j) C. Thibaudeau; J. Plavec and J. Chattopadhyaya *J. Org. Chem.* **1996**, *61*, 266.
5. (a) See ref. 17 in 4f. (b) S. Brahms; V. Fritsch; J.G. Brahms and E. Westhof *J. Mol. Biol.* **1992**, *223*, 455.
6. R.M. Izatt; J.J. Christensen and J.H. Rytting *Chem. Rev.* **1971**, *71*, 439.